New BIOTECHNOLOGY 61 (2021) 29–39

Contents lists available at ScienceDirect

New BIOTECHNOLOGY

journal homepage: www.elsevier.com/locate/nbt

Two new exopolysaccharides from a thermophilic bacterium *Geobacillus* sp. WSUCF1: Characterization and bioactivities

Jia Wang [a,d], David R. Salem [a,b,c,*], Rajesh K. Sani [a,c,d,*]

[a] Department of Chemical and Biological Engineering, South Dakota School of Mines and Technology, Rapid City, SD, 57701, USA
[b] Department of Materials and Metallurgical Engineering, South Dakota School of Mines and Technology, Rapid City, SD, 57701, USA
[c] Composite and Nanocomposite Advanced Manufacturing Center - Biomaterials (CNAM-Bio Center), Rapid City, SD, 57701, USA
[d] BuG ReMeDEE Consortium, South Dakota School of Mines and Technology, Rapid City, SD, 57701, USA

ARTICLE INFO

Keywords:
Thermophile
Geobacillus
Exopolysaccharide
Thermostability
Non-cytotoxicity
Antioxidancy

ABSTRACT

The production, characterization and bioactivities of exopolysaccharides (EPSs) from a thermophilic bacterium *Geobacillus* sp. strain WSUCF1 were investigated. Using glucose as a carbon source 525.7 mg/L of exoproduct were produced in a 40-L bioreactor at 60 °C. Two purified EPSs were obtained: EPS-1 was a glucomannan containing mannose and glucose in a molar ratio of 1:0.21, while EPS-2 was composed of mannan only. The molecular weights of both EPSs were estimated to be approximately 1000 kDa, their FTIR and NMR spectra indicated the presence of α-type glycosidic bonds in a linear structure, and XRD analysis indicated a low degree of crystallinity of 0.11 (EPS-1) and 0.27 (EPS-2). EPS-1 and EPS-2 demonstrated high degradation temperatures of 319 °C and 314 °C, respectively, and non-cytotoxicity to HEK-293 cells at 2 and 3 mg/mL, respectively. In addition, both showed antioxidant activities. EPSs from strain WSUCF1 may expand the applications of microorganisms isolated from extreme environments and provide a valuable resource for exploitation in biomedical fields such as drug delivery carriers.

Introduction

The demand for natural polymers continues to increase as alternatives to synthetic polymers are sought, in order to avoid the undesirable toxicity and lack of biodegradability of petroleum-based polymer waste streams. Plant polysaccharides represent a large portion of the natural carbohydrate polymers currently used in various industrial sectors. However, the immense diversity in molecular structure and chemical composition of microbial exopolysaccharides (EPSs) can result in a much greater variety of physico-chemical properties and biological activities than are available in polysaccharides of plant origin. Several microbial EPSs, such as xanthan, dextran and gellan, have already been widely applied in food industries, [1], and increased exploration of microbial EPSs provides an important opportunity for the replacement of some synthetic polymers [2].

Extreme environments can provide an invaluable resource for microorganisms defined as extremophiles and their bioproducts, such as thermostable enzymes and biopolymers [2–4]. As an extremophile type, thermophilic bacteria produce different kinds of macromolecules, including EPSs, as adaptations to assist the microbial communities to endure extremes of temperature, and their biomolecules are considered to have great advantages compared with those from mesophilic microorganisms [5,6]. It has been revealed that thermophilic EPSs have important potential arising from their thermostability and biological activities, including biocompatibility, antioxidant properties, non-cytotoxicity, anti-viral and immunostimulant effects [2,7,8]. Thermophilic bacteria are more likely to be applied as cell factories to produce industrially significant EPSs due to their lack of pathogenicity and short period of productivity [9].

Thermophilic *Geobacillus* spp. are widely distributed in geothermal areas such as hot springs and hydrothermal vents, and they usually perform fast growth in comparatively simple media with inexpensive

Abbreviations: ANOVA, one-way analysis of variance; CASPER, computer assisted spectrum evaluation of regular polysaccharides; DMSO, dimethyl sulfoxide; DPPH, 22-diphenyl-1-picrylhydrazyl; DTG, derivative thermogravimetry; EPS, exopolysaccharide; FTIR, Fourier-transform infrared spectroscopy; HPLC, high performance liquid chromatography; MTT, 3−45-dimethylthiazol-2-yl)-2,5-diphynyltetrazolium bromide; NMR, nuclear magnetic resonance; T_d, degradation temperatures; TFA, trifluoroacetic acid; TGA, thermogravimetric analysis; XRD, X-ray diffraction.

* Corresponding authors at: Department of Chemical and Biological Engineering, South Dakota School of Mines and Technology, Rapid City, SD, 57701, USA.
E-mail addresses: David.Salem@sdsmt.edu (D.R. Salem), Rajesh.Sani@sdsmt.edu (R.K. Sani).

https://doi.org/10.1016/j.nbt.2020.11.004
Received 31 March 2020; Received in revised form 6 November 2020; Accepted 7 November 2020
Available online 11 November 2020

carbon and nitrogen sources [5,10,11]. In recent years, they have been characterized and identified as potential producers of EPSs with a wide range of physicochemical and biological properties, which may rarely be found in more traditional polymers [1]. These studies have indicated that *Geobacillus* spp. are a promising resource for production of novel thermophilic EPSs with unique properties and bioactivities for future biotechnological and biomedical applications. However, such candidate thermophilic EPSs have been insufficiently accumulated, leading to limited knowledge of the *Geobacillus* spp. EPS-producers and their industrial potential. The characterization and description of biological activities of novel EPSs they produce are necessary in order to provide more EPS candidates with prospective commercial value. The low yield of EPSs produced by *Geobacillus* spp. is another restriction to the extension of their commercial applications. Optimization and further scale-up of EPS fermentation by *Geobacillus* sp. strains will therefore be advantageous in attaining economical production processes. Furthermore, the discovery of new EPS-producers from the *Geobacillus* spp. may provide more substantial information to assist in the elucidation of the biological mechanisms and structure-property relationship of thermophilic EPSs.

Thermophilic bacterium *Geobacillus* sp. WSUCF1 was isolated from the sample obtained from a compost facility, and is known to produce highly thermostable lignocellulolytic enzymes [12]. This strain demonstrated primary EPS-producing capability using various monosaccharides and disaccharides as carbon source, and the putative mechanism of its EPS biosynthesis and export has been reported through genome annotation using its draft genome [6]. The aim of the present study was to optimize the cultivation approach for EPS production by WSUCF1 and determine the characteristics and bioactivities of its synthesized EPS.

Material and methods

Microorganism and culture conditions

Geobacillus sp. strain WSUCF1 was originally isolated from sample collected from a compost facility at Washington State University, Pullman, WA [12]. For EPS production, it was inoculated from an agar plate and grown in 250-mL Erlenmeyer flasks with 50 mL liquid medium and cultured in a shaking incubator at 60 °C, 180 rpm for 24 h as preculture. The preculture was then inoculated (5%, v/v) into 1000-mL Erlenmeyer flasks with 300 mL liquid medium and cultured in a shaking incubator at 60 °C, 180 rpm for 24 h. The basal medium contained glucose, 6.0 g/L, yeast extract, 1.0 g/L and NaCl, 3.0 g/L, and the initial pH was adjusted to 7.0 by 1 M NaOH. The medium was sterilized at 121 °C for 15 min.

Enhancement of EPS production

In a previous study, glucose was found to be the optimum carbon source leading to relatively higher EPS production compared with other mono and disaccharides and was the carbon source in this study [6]. EPS production was further analyzed using other nitrogen sources, including peptone and beef extract at 1.0 g/L in a basal medium (glucose 6.0 g/L, peptone or beef extract 1.0 g/L, and NaCl 3.0 g/L). By growing the strain in the presence of the favored carbon and nitrogen source, the influence of other variables was tested step-by-step in the following order: temperature, pH value, concentration of nitrogen source, concentration of carbon source, and concentration of NaCl. At each step, the optimum results obtained from the previously examined parameter were retained. EPS and biomass content were measured according to the analytical methods below. All the experiments were performed in triplicate and averaged data were reported.

Scale-up fermentation in a bioreactor

The large-scale production of EPS by strain WSUCF1 was carried out in a 40-L bioreactor (New Brunswick™ BioFlo® 510 Fermentor, Eppendorf, Inc., Hauppauge, NY, USA) with working volume of 20 L using optimized liquid medium of glucose 6.0 g/L, yeast extract 20.0 g/L and NaCl 3.0 g/L sterilized *in situ*. The initial pH was adjusted to 7.0 by 6 M NaOH before autoclaving. A 5% (v/v) of WSUCF1 from preculture was transferred into bioreactor. During the fermentation, the temperature was maintained at 60 °C, and the pH was measured and allowed to vary according to the metabolites produced without correction. The bioreactor was operated in batch mode and aerated at 2 vvm with constant agitation at 200 rpm for 24 h. Microbial growth and EPS production were monitored quantitatively by sampling 20 mL of culture broth [2].

Analytical methods

The microbial biomass was measured in terms of optical density (OD) at 600 nm using the corresponding medium as blank. For cell dry weight (CDW) determination, the fermentation broth was centrifuged at 6000 *g* for 15 min, and the wet cell pellets were recovered. The bacterial cells were washed with normal saline, centrifuged and dried at 60 °C to a constant weight. To convert OD value to CDW, a calibration curve of biomass concentration *versus* OD was prepared by plotting the CDW against OD_{600}. The maximum specific growth rate (μ_{max}) was calculated from the slope of the natural log of CDW *versus* time plots in the exponential phase through linear regression. For EPS quantification, the cell-free supernatant was mixed with an equal volume of chilled absolute ethanol (−20 °C) added dropwise under stirring in an ice bath. The alcoholic solution was kept at −20 °C overnight and then centrifuged at 8000 *g* for 40 min. The pellet was dissolved in a minimum volume of deionized water. The carbohydrate content of the pellet was assayed by the phenol-sulfuric acid method using glucose as standard [13]. The protein content was estimated using Bradford reagent (Thermo Scientific, Rockford, IL, USA) with bovine serum albumin as standard [14]. The nucleic acid content was measured using a NanoDrop ND-1000 spectrophotometer (Thermo Scientific, Wilmington, DE, USA) at the wavelength of 260 nm. The same procedure was also carried using the uninoculated medium as a control. The carbohydrate, protein and nucleic acid contents of EPS were calculated subtracting the corresponding values of blank medium when necessary. Uronic acid content was determined according to the method described in [15] using galacturonic acid as standard. The metabolites were analyzed in cell-free culture supernatant using HPLC as described previously [16].

Isolation and purification of EPS

The bacterial cells were removed by centrifugation at 6000 *g* for 15 min. Proteins in cell-free supernatant were precipitated by adding ammonium sulfate to 100% (w/v) saturation, and removed by centrifugation at 10,000 *g* for 30 min, followed by dialysis against deionized water. Subsequently, one volume of chilled absolute ethanol (−20 °C) was added to one volume of supernatant dropwise under stirring in an ice bath, and the mixture was incubated at −20 °C overnight. The precipitate as crude EPS was harvested by centrifugation (8000 *g*, 40 min), dissolved in a minimum amount of deionized water, and then dialyzed against deionized water for 3 d at 4 °C.

The crude EPS was purified using DEAE Sepharose CL-6B column (1.9 × 60 cm). Crude EPS (20 mg/mL) was eluted first with 100 mL deionized water, followed by a discontinuous NaCl gradient (100 mL at each NaCl concentration) from 0.1 to 1.0 M with an increment of 0.1 M at a flow rate of 0.2 mL/min. Each elution fraction (10 mL) was collected and the EPS content was assayed by the phenol-sulphuric acid method [13]. Each fraction containing a carbohydrate component was combined, concentrated by rotary evaporator, and then further purified by Sephadex G-50 column (2.5 × 50 cm) using deionized water as eluent with a flux of 0.5 mL/min. The fractions with EPS were pooled and evaporated before being applied for further characteristic analysis.

EPS characterization

Monosaccharide analysis

The purified EPS was hydrolyzed by 2 M trifluoroacetic acid (TFA) at 120 °C for 2 h in a sealed vial and then vacuum-dried. The hydrolysate was used for the quantification of the constituent monosaccharide monomers using HPLC as described previously [16]. Monosaccharide identification was determined by comparison with standard monosaccharides, namely glucose, mannose, galactose, fructose, rhamnose, xylose, and arabinose. Pyruvic acid content was detected by the method reported in [17]. The presence of sulfate was investigated as in [18].

Molecular weight

The molecular weight of purified EPSs was estimated by gel filtration on a Sepharose CL-6B column (1.9 × 80 cm) using deionized water as eluent with flow rate of 0.1 mL/min. Each fraction (2 mL) was tested for the presence of carbohydrate by phenol-sulphuric acid method. A series of dextran standards (150, 270, 410, 670 and 1100 kDa) were assayed under the same conditions and a calibration curve was obtained by plotting the elution volume *versus* the $\log_{10}$ of the corresponding molecular weight.

FTIR and NMR spectroscopy

The infrared spectrum of EPS was recorded at room temperature (RT) using an Agilent Cary 600 FTIR spectrometer (Agilent Technologies, Santa Clara, CA, USA). The EPS sample was mixed with dry KBr powder in the ratio of 1:50 (w/w), ground and then pressed into pellet for FTIR measurement in the frequency range of 4000 to 400 cm^{-1}. The NMR spectrum of the EPS sample was recorded at 300 (^{1}H) or 75 MHz (^{13}C) on a Bruker Avance-II 300 spectrometer (Bruker BioSpin, Karlsruhe, Germany) in D_2O (40 mg/mL) at RT. Chemical shifts were reported in parts per million (ppm) with reference to acetone for ^{1}H and ^{13}C-NMR spectra.

Thermogravimetric analysis

Thermogravimetric analysis (TGA) of EPS was conducted by using a TA Q600 TGA apparatus (TA Instruments Inc., New Castle, DE, USA). EPS sample (approximately 5 mg) was sealed in an aluminum pan and heated from 20 to 600 °C at a heating rate of 10 °C/min under nitrogen atmosphere with a flow of 20 mL/min. The empty aluminum pan was applied as a reference.

X-ray diffraction (XRD) analysis

X-ray diffraction (XRD) was performed on an Ultima-Plus X-ray powder diffractometer (Rigaku Co. Ltd., Tokyo, Japan), using CuK_{α} irradiation. The crushed sample was placed on a sample holder at RT and the diffractometer was operated at 40 kV and 40 mA. The diffractogram was recorded at 2θ angles between 3° to 60° with a scan speed of 2° per minute. The *d*-spacing at the value of θ was calculated by Bragg's law, and the crystallinity index was calculated from the area under crystalline peaks normalized with respect to total scattering area.

Cytotoxicity assay

Human embryonic kidney-293 (HEK-293) cells (ATCC CRL-1573) were kindly provided by Dr. Jing Liu, Indiana University - Purdue University Indianapolis, Indianapolis, IN, USA. They were maintained in Dulbecco's modified Eagle's medium (DMEM) supplemented with 10 % fetal bovine serum, 50 μg/mL penicillin and 50 μg/mL streptomycin at 37 °C in an atmosphere of 5% CO_2. For the cytotoxicity test, 200 μL media containing 8×10^3 HEK-293 cells per well were seeded separately into 96-well microtiter plate, and incubated for cell adherence for 24 h at 37 °C in an atmosphere of 5% CO_2. After incubation, the culture supernatant was removed. The adherent cells were exposed to a concentration range of 500–10000 μg/mL of EPS dissolved in DMEM and incubated for 24 h at 37 °C in an atmosphere of 5% CO_2. Then 10 μL (3-(4,5-dimethylthiazol-2-yl)-2,5-diphynyltetrazolium bromide (MTT) solution (Biotium Inc., Hayward, CA, USA) was added to each well and the plate incubated at 37 °C for 4 h. After incubation, the culture supernatant containing MTT from each well was removed, and 200 μL dimethyl sulfoxide (DMSO) was added to each well to dissolve formazan crystals. Absorbance was measured at 570 nm with a reference wavelength of 660 nm using a multi-mode microplate reader (EPOCH 2, BioTek, Winooski, VT, USA). DMEM without EPS was used as negative control which was considered 100% viable. The percentage of cell viability was calculated according to: viability (%) = (absorbance of cells treated with EPS/absorbance of negative control) × 100%. All experiments were performed in triplicate.

Antioxidant activity in vitro

The free radical scavenging activities of purified EPSs against hydroxyl radical ($^{\bullet}OH$), 1,1-diphenyl-2-picryl-hydrazyl radical (DPPH$^{\bullet}$), and superoxide anion radical ($O^{2-\bullet}$) were evaluated mainly according to the method of [19], described in detail in the supplementary information.

Statistical analysis

The experimental data were expressed as mean value ± standard error calculated from three parallel experiments. The statistical analysis was performed by one-way analysis of variance (ANOVA) using Microsoft Excel. Differences were regarded as significant when $p < 0.05$.

Results and discussion

Enhancement of EPS production

The one-factor-at-a-time strategy for EPS production by *Geobacillus* sp. strain WSUCF1 was applied starting from the basic medium with glucose as a carbon source. The carbohydrate concentration quantified by the phenol-sulfuric acid method in the ethanol precipitated pellet was taken to represent EPS productivity. To investigate the suitable nitrogen source for EPS production, three complex nitrogen sources were tested in the basal medium, and the results demonstrated that WSUCF1 could only produce significant amounts of EPS with yeast extract (Fig. 1a). Although the level of growth of WSUCF1 was also significant with tryptone as nitrogen source, EPS production was not proportional to it. The application of complex nitrogen sources usually provides higher specific growth rate and EPS production [20]. The stimulatory effect of yeast extract may be due to its high content of short peptides, free amino acids and growth factors [21]. Both the maximum cell growth and EPS production were observed at 60 °C, and tended to deteriorate as the culture temperature either increased or decreased (Fig. 1b). The optimal pH value for both cell growth and EPS production was found to be about pH7 (Fig. 1c). The initial medium pH has been considered to affect cell membrane function, cell morphology and structure, and the uptake of nutrients [22]; it may also relate to the stability and activity of the enzymes involved in EPS biosynthesis [23]. Unlike mesophilic EPS-producing bacteria, which may need sub-optimal growth conditions for increased EPS yield, the favorable pH and temperature for thermophilic EPS production are usually identical with the optimum conditions for growth.

Under the optimized conditions, the growth of WSUCF1 increased prominently when yeast extract concentration was higher than 4 g/L (Fig. 1d). Yeast extract had a significantly positive effect on EPS production, and the optimum concentration was about 20 g/L. While optimizing the process, it was determined that the polysaccharides were not derived from the yeast extract present in the medium. The control medium without inoculation was tested for polysaccharide content as a reference by the same EPS analysis methods. The carbohydrate concentrations after ethanol precipitation of the control medium were considered as background and were subtracted from the total carbohydrates in the sample containing the microbially produced EPS, giving the total amount of microbially produced EPS as the reported value. Several

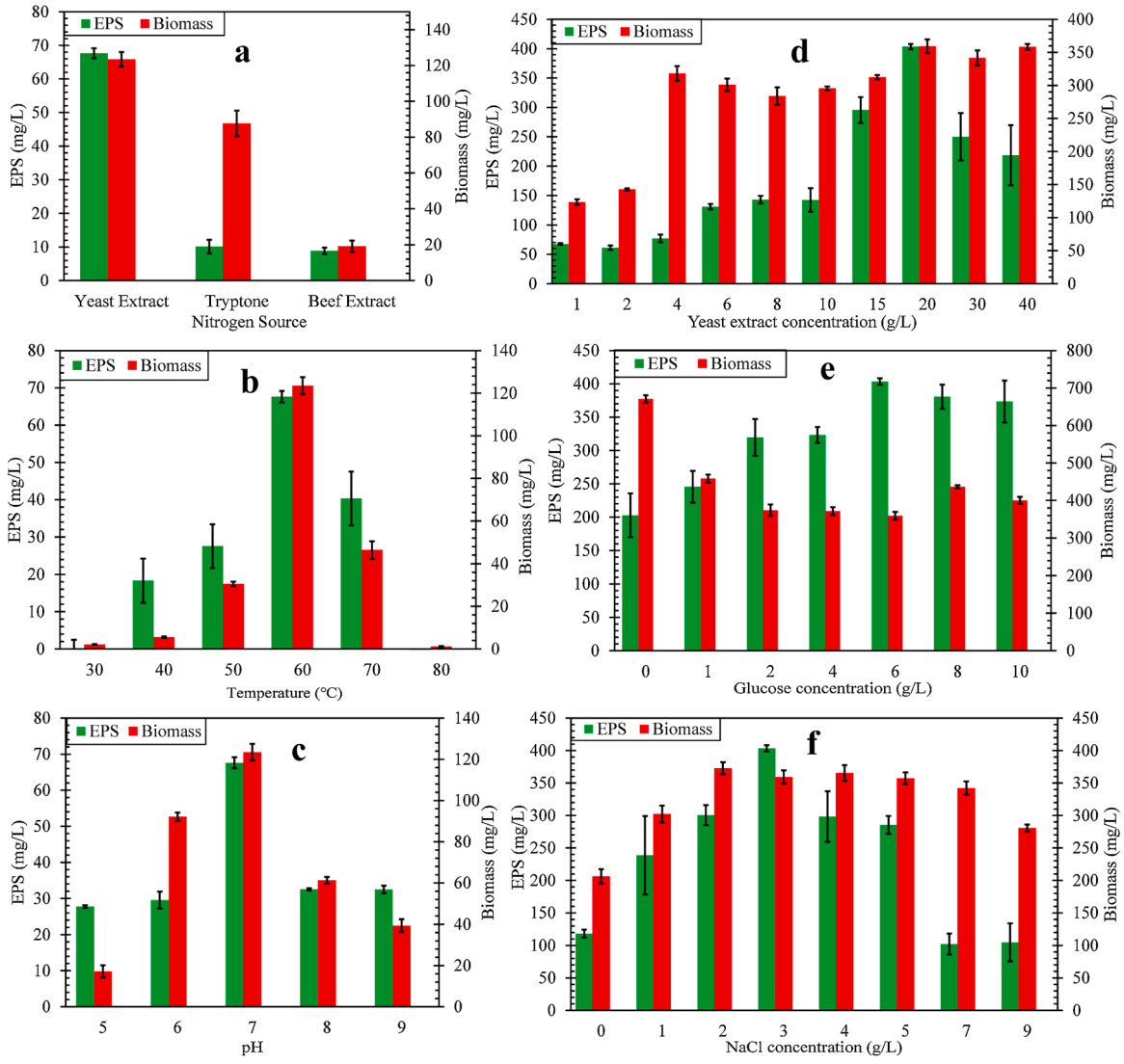

Fig. 1. Effect of (a) nitrogen sources, (b) temperature, (c) pH value, (d) yeast extract concentration, (e) glucose concentration, and (f) NaCl concentration on the growth and EPS production by WSUCF1. Columns: Total biomass (red); EPS (green). The biomass is represented by cell dry weight concentration in the medium. The presented data are means of three replicates, with standard errors shown.

bacteria have been reported to produce optimum amounts of EPS using high concentration of yeast extract in the growth medium. Lactic acid bacterium *Weissella confuse* OF126 produced branched α-glucan EPS with a molecular weight of 1100 kDa at an optimum concentration of 25 g/L yeast extract in growth medium [24]; both *Lactobacillus plantarum* strains YO175 and OF101 utilized 25 g/L yeast extract as their most effective nitrogen source for EPS production [25]; another lactic acid bacterium, L. *plantarum* MTCC 9510 generated glucomannan using 40 g/L yeast extract. The productivity of EPS when using a high content of yeast extract was not due to the interference of carbohydrates present in yeast extract, since the polysaccharides in the medium were found to be negligible [26]. A marine bacterium *Streptococcus phocae* also produced the maximum yield of an EPS composed of arabinose, fructose and galactose using 20 g/L yeast extract without any contamination from yeast extract [21]. *Bordetella* sp. B4 produced a glucan-type EPS with 20 g/L yeast extract in the medium [27]. The causes and effects of many environmental parameters on EPS production remain open for debate due to observed inconsistencies across various kinds of organisms (*e.g.* mesophiles, neutrophiles, and extremophiles). In this study, it appears that the growth of WSUCF1 on a medium with a rich complex nitrogen source is beneficial to EPS production, and the improvement may be correlated with the increase of cell growth. It is suggested that this might be attributed to a lower energy requirement to achieve the same biomass concentration with a high complex nitrogen source concentration, leaving more energy available for EPS biosynthesis [28].

As shown in Fig. 1e, a gradual increase in glucose from 2 to 10 g/L did not lead to a significant increase in biomass or EPS production. Optimum EPS production was attained at 6 g/L glucose; thereafter WSUCF1 could grow at NaCl concentrations from 1 to 9 g/L, and the maximum EPS production appeared at 3 g/L (Fig. 1f). When NaCl was 7 and 9 g/L, EPS production was relatively inhibited. For a non-halophilic bacterium, the osmotic pressure caused by a high NaCl concentration may be disadvantageous to metabolite biosynthesis, even though cell growth was not inhibited [29]. In summary, optimization of the culture medium led to an increase of EPS production from 68 to 404 mg/L, using a complex medium with a relatively simple composition.

Large-scale EPS production in bioreactor

For bioreactor cultivation, a 40 L fermenter with 20 L working volume was used and cultivation was performed under optimum culture medium (glucose 6.0 g/L, yeast extract 20.0 g/L, and NaCl 3.0 g/L) and environmental conditions. The time course revealed that EPS production started with a logarithmic phase and continued to increase until the late stationary phase, with maximum achieved in the stationary phase after 12 h cultivation (Fig. 2). Maximal EPS production of 526 mg/L with a specific EPS yield of 0.66 mg/mg cell dry weight was obtained, while bacterial growth reached 803 mg/L by 10 h. The maximum specific growth rate μ_{max} was 0.69 h^{-1} during the exponential phase. Among the *Geobacillus* spp. EPS producers, WSUCF1 stands out for its higher capability of EPS production (Appendix A. Table S1 in supplementary information). Acetate, propionate and ethanol were detected as minor end products during EPS production (data not shown), and were also found as metabolites of several other *Geobacillus* sp. strains under aerobic conditions [30–33].

Purification of EPS

Using optimal medium, the crude EPS obtained through ethanol precipitation of the cell-free fermentation broth contained 84% (w/w) carbohydrate. It was purified through an anion exchange column, *e.g.* DEAE Sepharose CL-6B. The elution profile showed two major peaks (Fig. 3); the first EPS peak (EPS-1) was eluted in neutral conditions, and the second (EPS-2) at 0.1 M NaCl, suggesting that EPS-1 is a neutral polysaccharide while EPS-2 is acidic. There were also two minor peaks which eluted at higher concentration of NaCl, but their carbohydrate content was in both cases <10% (w/w). The pellet obtained by the same procedure from the blank medium without inoculation was also loaded onto the ion exchange column and no peaks were observed during elution. The two major EPS fractions were collected, concentrated and further purified and desalted through a gel filtration column (Sephadex G-50); each exhibited only a single peak, indicating that both were at qualified purity for further characterization.

It is not unusual to find that thermophilic *Geobacillus* spp. bacteria can produce more than one kind of purified EPS with different charge properties. The purification of the crude EPS produced by thermophilic bacterium *G. thermantarcticus* also showed two major EPS fractions [34]; *G. thermodenitrificans* B3−72 produced a major EPS fraction with negative charge and a minor neutral fraction [8,35]. *Geobacillus* sp. 4004 generated 3 fractions of EPS, with the major one also negatively charged [11]. The production of multiple EPSs with different structure and properties in thermophilic *Geobacillus* sp. strains indicates that more than one EPS gene cluster may be involved during EPS biosynthesis [1].

EPS characterization

Chemico-physical characterization

The total carbohydrate content was 95.6% (w/w) for EPS-1 and 92.7 % (w/w) for EPS-2, indicating that the main component of both was a polysaccharide (Table 1). The monosaccharide components were identified as mannose and glucose for EPS-1, while EPS-2 contained only mannose. Thus, the EPSs synthesized by WSUCF1 were biopolymers with glucomannan and mannan like structures. The molecular weights (MW) were estimated by gel filtration chromatography using a calibration curve derived from dextrans with standard MWs. The elution profile of EPS-1 and EPS-2 both demonstrated a single major fraction with a MW of approximately 1000 kDa.

Structural characterization

The FTIR spectra of EPS-1 and EPS-2 exhibited a broad peak at 3600 to 3000 cm^{-1} associated with the stretching vibration of the O—H bond (Fig. 4). Two absorption peaks at 2900 to 2800 cm^{-1} were attributed to the asymmetrical C—H stretching bands in a pyranose ring of constituent sugar residues. The peaks at 2200 to 2000 cm^{-1} represented aliphatic C—H bonds [36]. The evident absorbance at 1643 cm^{-1} and 1543 cm^{-1} in the EPS-2 spectrogram indicated the presence of amide I (carbonyl) and amide II (N—H) bonds [37]. Signals at 1385 cm^{-1} in both EPS-1 and EPS-2 spectrograms were indicative of C—H deformation oscillation [38]. The intense absorption within the 1150−950 cm^{-1} region was dominated by the glycosidic linage C—O—C contribution, and the FTIR peak of the glycosidic bond was at a frequency around 1025 cm^{-1} for EPS-1 and EPS-2. The sharp anomeric peak at 810 cm^{-1} revealed that the α-anomeric configuration of mannose could be the monomer units of both EPSs produced by WSUCF1 [39,40].

The pattern of FTIR absorption features for both EPS-1 and EPS-2 are typical of polysaccharides. The shoulders at 1126 and 972 cm^{-1} within the broad peak of the glycosidic bond may be from the stretching vibrations of the C—OH side groups and C—C stretching vibrations of pyranose ring, and they may relate to the α-(1,3)-type glycosidic link. The relatively low absorbance peaks in the region of the C—O—C glycosidic bond also indicates less diversity of the monomers [37,41]. Furthermore, no strong absorption peaks were found at 1260 to 1220 cm^{-1}, indicating the absence of sulfate groups such as S═O or C—O—S

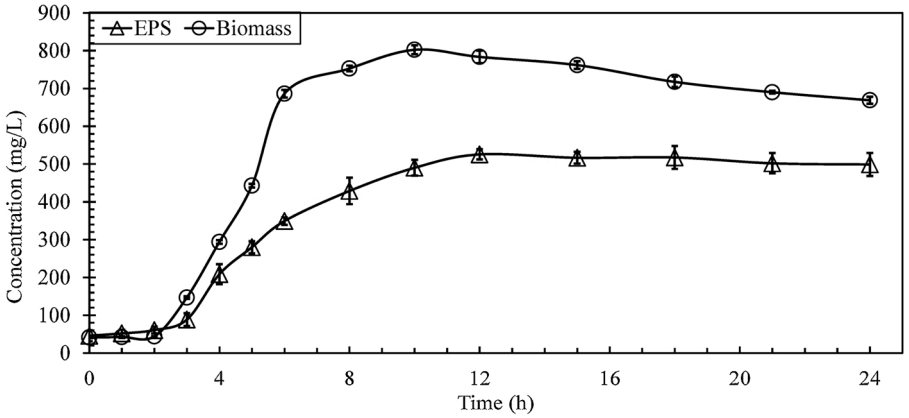

Fig. 2. Time course of growth and EPS production by WSUCF1 in bioreactor. Symbols: Total biomass (circles); EPS (triangles). The biomass is transferred as cell dry weight concentration in the culture medium. Values are means of three replicates with standard error bars shown, except where smaller than the symbols.

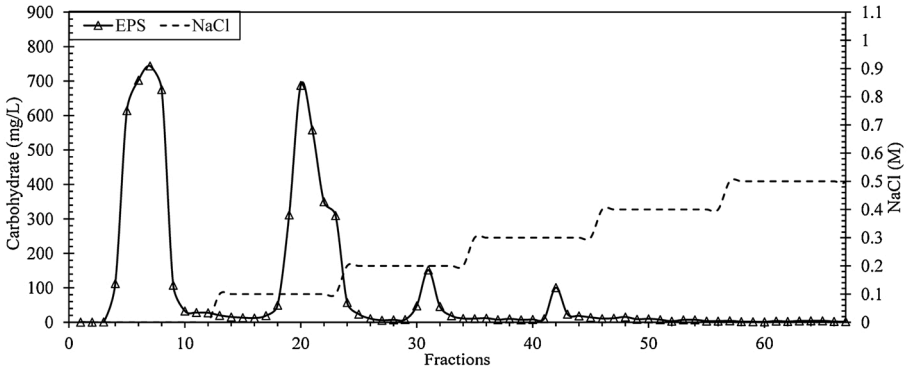

Fig. 3. Purification profile of crude EPS of WSUCF1 on DEAE Sepharose CL-6B column. The EPS content is represented by triangles for each fraction, and the NaCl concentration of elution buffer is represented by the dashed line. Fractions eluted over 0.5 M NaCl contained no carbohydrate and are not shown.

Table 1
Chemical-physical characterization of EPSs from *Geobacillus* sp. WSUCF1.

Properties	EPS-1	EPS-2
Carbohydrate content (%, w/w)	93.3	92.7
Protein content (%, w/w)	2.1	3.3
Nucleic acid content (%, w/w)	0.3	1.2
Uronic acid (%, w/w)	2.0	2.8
Monosaccharide composition (by molar ratio)	Mannose/glucose (1/0.21)	Mannose
Pyruvic acid (%, w/w)	2.3	Not detected
Molecular weight (kDa)	~1000	~1000
Degradation temperature (°C)	319	314

[37]. The weak peaks around 900 cm^{-1} may be due to the vibrations from phosphodiester bonds, indicating low content of nucleic acids in both EPSs [42].

The structures of EPS-1 and EPS-2 were further investigated by ^{1}H and ^{13}C NMR analyses. The ^{1}H NMR spectrum of EPS-1 showed four resonances in the anomeric region at δ 5.29, 5.12, 5.04 and 4.90 ppm (Fig. 5a). For EPS-1 those four anomeric peaks were assigned to the proton resonances of mannose and glucose as building blocks of EPS-1. The peak at δ 5.04 ppm could be from an α-(1,3)-linked non-reducing terminus, that at δ 5.12 ppm could be from an α-(1,3)-linked mannosyl unit at the main chain, and at δ 5.29 may be from an α-mannosyl unit at the reducing terminus [43]. Meanwhile, the signal obtained at δ 4.90 ppm indicates an α-(1,6)-glycosidic bond of glucose [24,44]. For EPS-2, the ^{1}H NMR spectroscopic data demonstrated three similar mannose anomeric peaks at δ 5.28, 5.14 and 5.05. The ring proton signals were also comparable with the putative mannose signals of EPS-1 (Table 2).

The ^{13}C NMR spectrum of EPS-1 showed the presence of two main anomeric carbons at δ 101.60 and 102.68 ppm, with other sugar ring carbons in the region of δ 60–80 ppm. The signal at δ 61.56 ppm was assigned to C-6 of mannose, and signal at δ 67.39 ppm of C-6 indicated the glucose units were linked by an α-(1,6) glycosidic bond. The glycosidic bond among mannose monomers was putatively considered as α-(1,3)-type. The ^{13}C NMR spectrum of EPS-2 had one anomeric sign at δ 102.36. Meanwhile, the C-6 signal was still at around δ 61 ppm indicating the exocyclic carbon C-6 was not linked by a glycosidic bond. From other ring carbon atom signals, the linkage in EPS-2 was tentatively assigned as an α-(1,3) glycosidic bond.

The chemical shifts of ^{1}H and ^{13}C NMR were uploaded and analyzed by the CASPER (Computer Assisted Spectrum Evaluation of Regular Polysaccharides) web server [45]. The predicted structure for EPS-1 was α-(1,3)-D-mannose and α-(1,6)-D-glucose, and for EPS-2 was α-(1,3)-D-mannose. ^{1}H and ^{13}C NMR chemical shifts simulated for the EPS-1 and EPS-2 structures using CASPER showed low deviation from the experimental results. The ^{13}C NMR spectrum of EPS-2 has six prominent resonances and no additional peaks in the region of anomeric carbon, indicating the absence of branched linkages in EPS-2 as mannan. Meanwhile, the ^{13}C NMR spectrum of EPS-1 had only two peaks in the region of anomeric carbon, indicating that it is also a glucomannan with linear structure. Due to the simplicity of the monosaccharide composition and non-branched molecular structures of the EPSs, the ^{1}H and ^{13}C NMR results could be compared with reported NMR data of linear glucomannan and mannan containing similar types of glycosidic linkage for assignments. It may be noted that recording the NMR data at RT, as performed here, is consistent with the protocol used for several exopolysaccharides with similar monosaccharide components [24,27,36,44,46,47].

Thermal properties and XRD analysis

TGA thermograms showed both EPS-1 and EPS-2 had a slight weight loss due to moisture evaporation between 80–120 °C, followed by rapid weight loss in the region from 260 to 320 °C, which is attributable to complex processes including the dehydration of the saccharide rings and depolymerization [48]. Degradation temperatures (T_d) of 319 and 314 °C were determined from the derivative curve (DTG) for EPS-1 and EPS-2, respectively (Appendix A. Fig. S1 in SI).

The industrial applications of EPS may significantly depend on its thermal behavior along with other physicochemical properties [49]. The thermal performance of EPSs produced by thermophilic strain *Geobacillus* sp. WSUCF1 displayed a resistance to temperatures that is remarkably higher than in other currently reported thermophilic EPSs [1]. This high thermostability may, for example, provide feasibility for biomedical applications requiring high temperature during manufacturing and processing.

The X-ray powder diffraction (XRD) is a powerful analytical technique for phase identification of materials [50], but to our knowledge has not been applied before to EPSs produced by thermophilic bacteria. The XRD profile of EPS-1 obtained from strain WSUCF1 exhibited a sharp and intense diffraction peak at 32.6° with inter planar spacing (*d*-spacing) of 0.275 nm, while EPS-2 has an intense diffraction peak at 31.7°, with a *d*-spacing of 0.282 nm (Fig. 6). The characteristic diffraction peak at around 32° was also observed for EPS produced by a mesophilic bacterium *Bacillus licheniformis* [51]. The XRD pattern indicated that both EPSs are predominantly amorphous in nature with a crystallinity index of 0.11 and 0.27 for EPS-1 and EPS-2, respectively. It is common for microbial EPSs to have a low degree of crystallinity [52] since abundant long side chains of the polymer, and the existence of

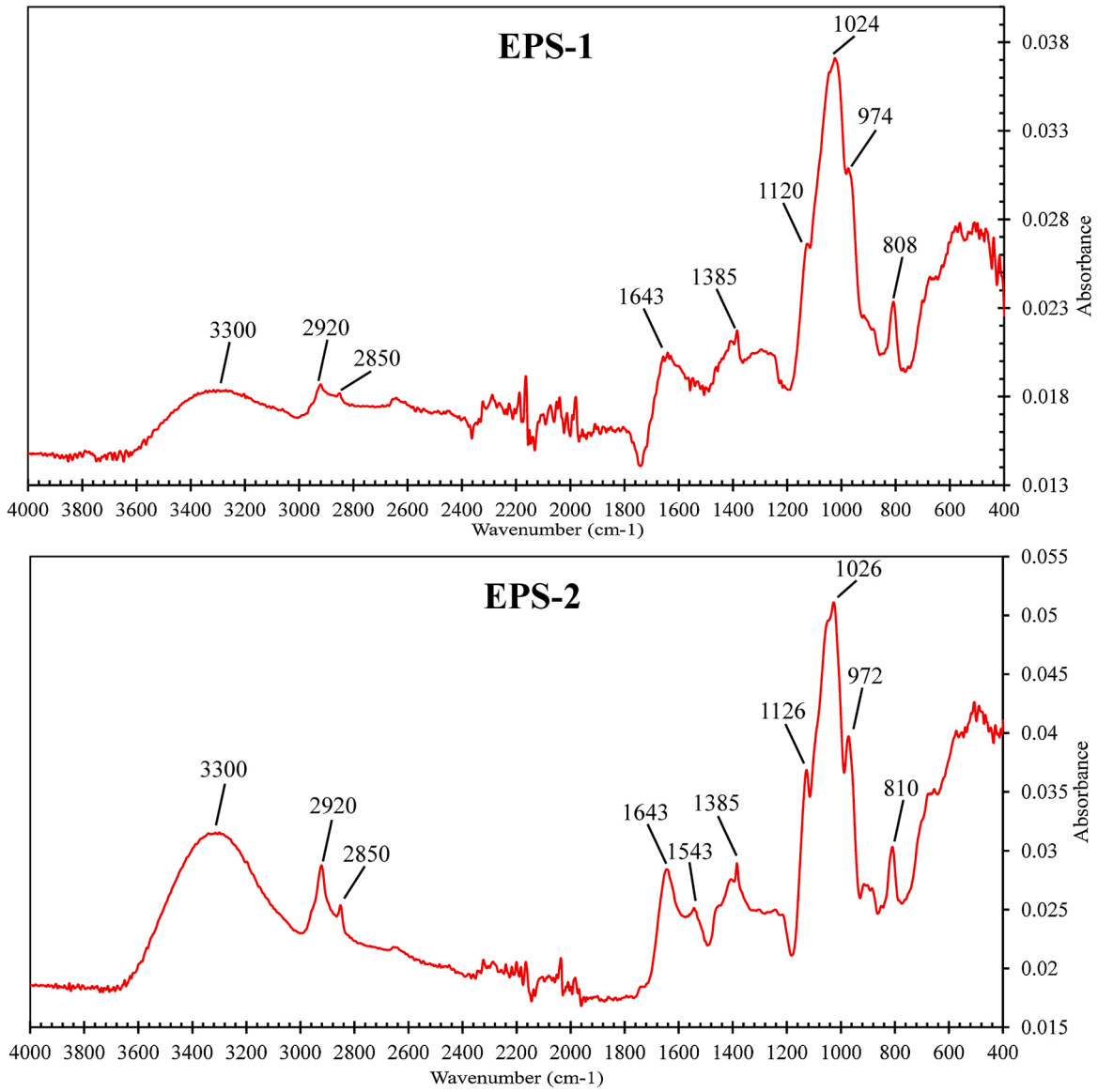

Fig. 4. FTIR spectra of the EPSs produced by WSUCF1. Spectra are demonstrated in absorbance mode for the two purified EPSs. The absorption peaks with annotation are shown.

different units and their irregular array, can all interfere with crystallization [53]. The homologous monosaccharide composition of EPS-2 might be related to its slightly higher crystallinity index compared with the that of EPS-1. However, the higher crystallinity of EPS-2 clearly did not result in any improvement in thermostability compared with EPS-1, as determined from TGA analysis.

Cytotoxicity of EPSs

The results of a cytotoxicity assay of the EPSs against HEK-293 cells revealed that even with at high concentrations (2 mg/mL of EPS-1 and 3 mg/mL of EPS-2), no significant effect on cell viability was observed (Fig. 7). These EPSs from thermophilic WSUCF1 showed non-cytotoxicity at relatively high concentrations compared with other extremophilic EPSs recently reported [8,9,54–57]. However, none of the cytotoxicity extremophilic EPSs was against HEK-293 cells, and very few exopolysaccharides from mesophilic bacteria were analyzed for cytotoxicity to HEK-293. The biocompatible nature of EPSs from WSUCF1 was better than that from mesophilic *L. mesenteroides* NRRL B-1426 which had no significant effect on the viability of HEK-293 cells at the concentration up to 1 mg/mL [58]. Another branched glucan-type EPS produced by mesophilic lactic acid organism *L. plantarum* DM5 also showed no cytotoxicity against HEK-293 cells at 1 mg/mL [59]. For polysaccharides, the degree of branching and chemical composition are considered to be highly related to their cytotoxicity [60]. The non-branched structure and simplicity of the monosaccharide composition of the EPSs from WSUCF1 may contribute to their biocompatibility. The non-cytotoxic property of bacterial EPSs makes them more appealing for biomedical applications compared with polysaccharides generated from plants and microalgae [9]. The superior biocompatibility of the thermophilic EPSs from WSUCF1 suggests their strong potential as safe biomaterials for biomedical products, such as drug carriers.

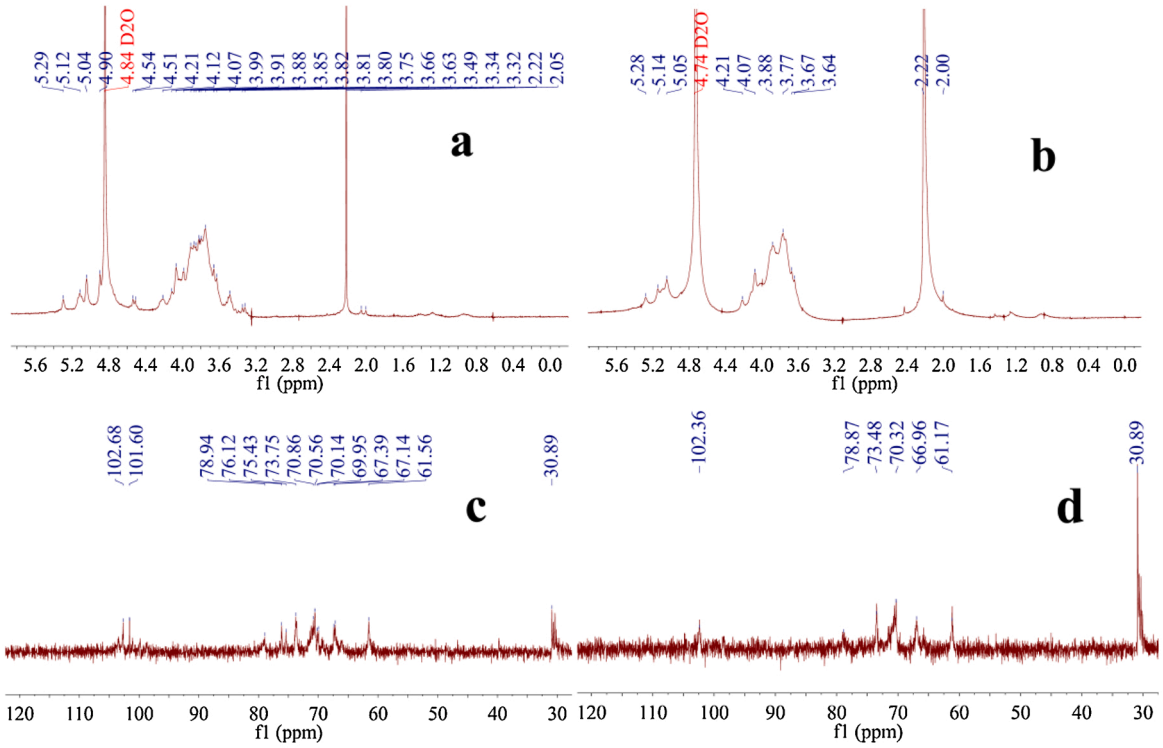

Fig. 5. ^{1}H-NMR spectra of (a) EPS-1 and (b) EPS-2, and ^{13}C-NMR spectra of (c) EPS-1 and (d) EPS-2 produced by WSUCF1. The solvent peaks are noted in red in the ^{1}H-NMR spectra. The NMR peaks with annotation are shown.

Table 2
Putative assignment of hydrogen and carbon chemical shifts based on ^{1}H and ^{13}C NMR spectroscopic data of EPS-1 and EPS-2.

	Chemical shifts (δ, ppm)					
	H-1 (anomeric) C-1	H-2 C-2	H-3 C-3	H-4 C-4	H-5 C-5	H-6, H-6' C-6
EPS-1						
Mannose	5.29/5.12/5.04	4.21	4.07	3.88	3.75	3.66/3.63
	102.68	70.56	78.94	67.14	73.75	61.56
Glucose	4.90	4.51	3.99	3.80	3.49	3.34/3.32
	101.60	75.43	76.12	70.14	70.86	67.39
EPS-2						
Mannose	5.28/5.14/5.05	4.21	4.07	3.88	3.77	3.67/3.64
	102.36	70.32	78.87	66.96	73.48	61.17

Antioxidant properties

From the antioxidant assay *in vitro*, EPS-1 showed moderate activities against DPPH and superoxide anion radicals at the dose of 10 mg/mL, which were superior to that of EPS-2 (Fig. 8a,b), while EPS-2 had more significant scavenging activity against hydroxyl radicals than EPS-1 at doses ranging from 1 to 10 mg/mL (Fig. 8c). The distinct antioxidant activities of these two EPSs present the possibility of selective performance against different free radicals. The chemical composition of the two EPSs may be related to their antioxidant properties, since glucose and mannose are common monosaccharide components in many polysaccharides with such activities [61]. Moreover, there is evidence that EPS with high content of uronic acid may have better radical scavenging properties [62]. Extremophilic EPSs with antioxidant activities are attractive as natural antioxidants for the prevention of oxidative damage in the body due to their non-pathogenicity [1]. It is possible that the EPSs from WSUCF1 with moderate antioxidant activities in this study

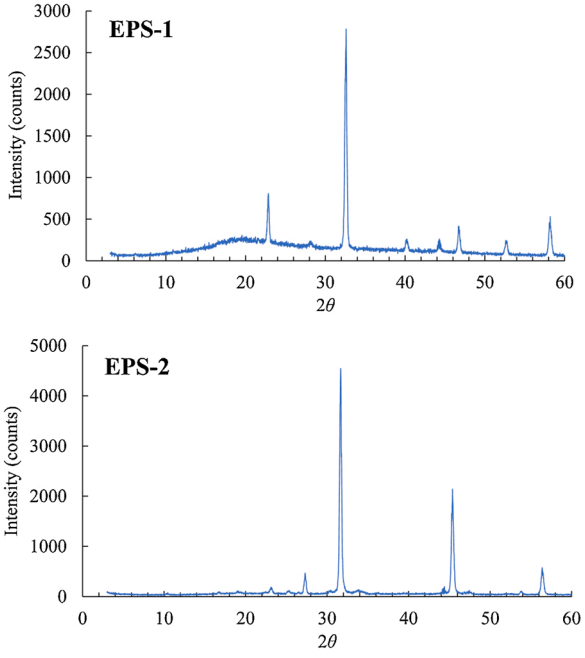

Fig. 6. XRD profile of EPSs obtained from WSUCF1. The XRD graphs show amorphous properties of the two purified EPSs.

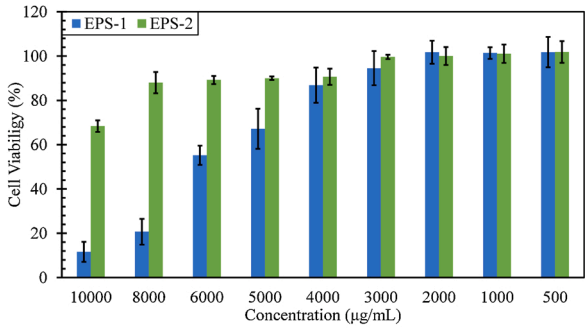

Fig. 7. Effect on HEK-293 cells of EPSs produced by WSUCF1. Columns: Cell viability treated by EPS-1 (blue); cell viability treated by EPS-2 (green). The presented data are means of three replicates, and standard errors are shown.

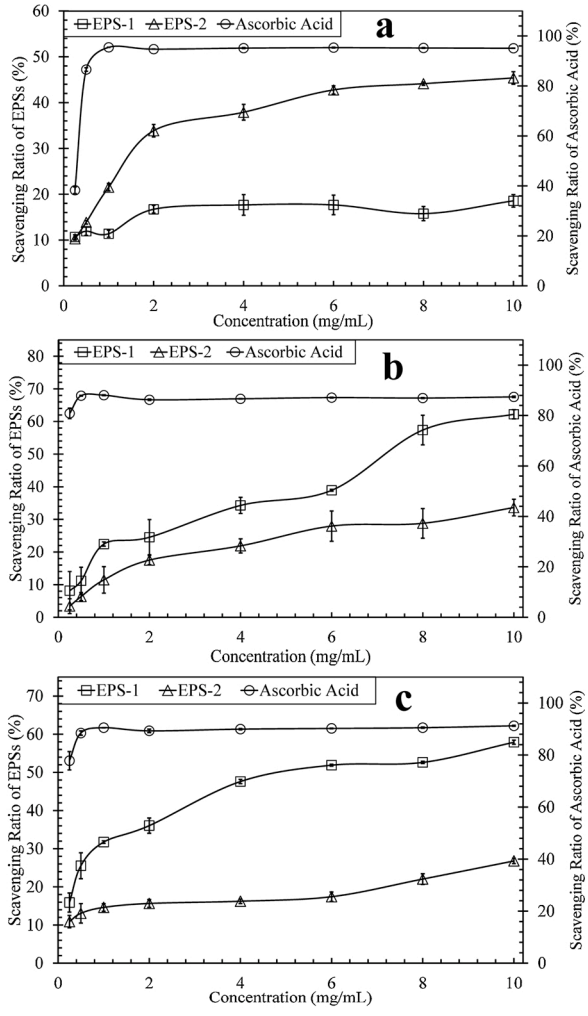

Fig. 8. Free radical-scavenging activities of EPSs from WSUCF1, (a) OH scavenging activity, (b) DPPH$^{\bullet}$ scavenging activity, and (c) $O^{2-\bullet}$ scavenging activity. Symbols: EPS-1 (square); EPS-2 (triangle); ascorbic acid (circle). The ascorbic acid was applied as a positive reference in free radical-scavenging test. Values are means of three replicates with standard error bars shown, except where smaller than the symbols.

could be further modified structurally to improve their antioxidant performance, based on guidance from the disclosure of structure-function relationships in antioxidant EPSs.

Conclusions

The thermophilic bacterium *Geobacillus* sp. WSUCF1 studied is among a limited number of reported *Geobacillus* species capable of producing significant amounts of EPSs. 526 mg/L EPS was produced with a specific yield of 0.66 mg EPS/mg cell dry weight in a 40-L bioreactor at 60 °C. Two EPSs were obtained and both had a molecular mass of approximately 1000 kDa. The monosaccharide and spectral analyses revealed that EPS-1 has a linear glucomannan-like structure with a backbone composed of α-(1,3)-linked mannose and α-(1,6)-linked glucose, and that EPS-2 has a linear mannan-like structure with α-(1,3)-linked mannose monomers. The observed outstanding thermostability and non-cytotoxicity of the EPSs are appealing for future exploration of their utilization in the biomedical industry. The antioxidant activities of these EPSs may also be considered as a potential resource in responding to the increasing demand for natural polysaccharides in biotechnological applications. Further research work is in progress on the development of EPS-antitumor drug-monoclonal antibody conjugates using these biocompatible EPSs as carriers for antitumor drug delivery with targeting function.

Declaration of Competing Interest

The authors report no declarations of interest.

Acknowledgements

This research was supported by the National Science Foundation in the form of BuG ReMeDEE initiative (Award # 1736255) and the Department of Chemical and Biological Engineering at the South Dakota School of Mines and Technology. Authors also gratefully acknowledge the financial support from the CNAM-Bio Center and "Proof of Concept" grant provided by the South Dakota Governor's Office of Economic Development.

Appendix A. Supplementary data

Supplementary material related to this article can be found, in the online version, at doi:https://doi.org/10.1016/j.nbt.2020.11.004.

References

[1] Wang J, Salem DR, Sani RK. Extremophilic exopolysaccharides: a review and new perspectives on engineering strategies and applications. Carbohydr Polym 2019; 205:8–26. https://doi.org/10.1016/j.carbpol.2018.10.011.

[2] Kambourova M, Mandeva R, Dimova D, Poli A, Nicolaus B, Tommonaro G. Production and characterization of a microbial glucan, synthesized by *Geobacillus tepidamans* V264 isolated from Bulgarian hot spring. Carbohydr Polym 2009;77: 338–43. https://doi.org/10.1016/j.carbpol.2009.01.004.

[3] Nicolaus B, Kambourova M, Oner ET. Exopolysaccharides from extremophiles: from fundamentals to biotechnology. Environ Technol 2010;31:1145–58. https://doi.org/10.1080/09593330903552094.

[4] Bhalla A, Bansal N, Kumar S, Bischoff KM, Sani RK. Improved lignocellulose conversion to biofuels with thermophilic bacteria and thermostable enzymes. Bioresour Technol 2013;128:751–9. https://doi.org/10.1016/j.biortech.2012.10.145.

[5] Gugliandolo C, Lentini V, Spanò A, Maugeri TL. New bacilli from shallow hydrothermal vents of Panarea Island (Italy) and their biotechnological potential. J Appl Microbiol 2012;112:1102–12. https://doi.org/10.1111/j.1365-2672.2012.05272.x.

[6] Wang J, Goh KM, Salem DR, Sani KR. Genome analysis of a thermophilic exopolysaccharide-producing bacterium - *Geobacillus* sp. WSUCF1. Sci Rep 2019;9: 1608. https://doi.org/10.1038/s41598-018-36983-z.

[7] Wang L, Zhang H, Yang L, Liang X, Zhang F, Linhardt RJ. Structural characterization and bioactivity of exopolysaccharide synthesized by *Geobacillus* sp. TS3-9 isolated from radioactive radon hot spring. Adv Biotech Micro 2017;4: 1–8. https://doi.org/10.19080/AIBM.2017.04.555635.

[8] Arena A, Gugliandolo C, Stassi G, Pavone B, Iannello D, Bisignano G, et al. An exopolysaccharide produced by *Geobacillus thermodenitrificans* strain B3-72: antiviral activity on immunocompetent cells. Immunol Lett 2009;123:132–7. https://doi.org/10.1016/j.imlet.2009.03.001.

[9] Yildiz SY, Anzelmo G, Ozer T, Radchenkova N, Genc S, Di Donato P, et al. *Brevibacillus themoruber*: a promising microbial cell factory for exopolysaccharide production. J Appl Microbiol 2014;116:314–24. https://doi.org/10.1111/jam.12362.

[10] Panosyan H, Di Donato P, Poli A, Nicolaus B. Production and characterization of exopolysaccharides by *Geobacillus thermodenitrificans* ArzA-6 and *Geobacillus toebii* ArzA-8 strains isolated from an Armenian geothermal spring. Extremophiles 2018; 22:725–37. https://doi.org/10.1007/s00792-018-1032-9.

[11] Moriello VS, Lama L, Poli A, Gugliandolo C, Maugeri TL, Gambacorta A, et al. Production of exopolysaccharides from a thermophilic microorganism isolated from a marine hot spring in flegrean areas. J Ind Microbiol Biotechnol 2003;30: 95–101. https://doi.org/10.1007/s10295-002-0019-8.

[12] Rastogi G, Bhalla A, Adhikari A, Bischoff KM, Hughes SR, Christopher LP, et al. Characterization of thermostable cellulases produced by *Bacillus* and *Geobacillus* strains. Bioresour Technol 2010;101:8798–806. https://doi.org/10.1016/j.biortech.2010.06.001.

[13] DuBois M, Gilles KA, Hamilton JK, Rebers PA, Smith F. Colorimetric method for determination of sugars and related substances. Anal Chem 1956;28:350–6. https://doi.org/10.1021/ac60111a017.

[14] Bradford MM. A rapid and sensitive method for the quantitation of microgram quantities of protein utilizing the principle of protein-dye binding. Anal Chem 1976;72:248–54. https://doi.org/10.1016/0003-2697(76)90527-3.

[15] Blumenkrantz N, Asboe-Hansen G. New method for quantitative determination of uronic acids. Anal Biochem 1973;54:484–9. https://doi.org/10.1016/0003-2697(73)90377-1.

[16] Wang J, Bibra M, Venkateswaran K, Salem DR, Rathinam NK, Gadhamshetty V, et al. Biohydrogen production from space crew's waste simulants using thermophilic consolidated bioprocessing. Bioresour Technol 2018;255:349–53. https://doi.org/10.1016/j.biortech.2018.01.109.

[17] Anthon GE, Barrett DM. Modified method for the determination of pyruvic acid with dinitrophenylhydrazine in the assessment of onion pungency. J Sci Food Agric 2003;83:1210–3. https://doi.org/10.1002/jsfa.1525.

[18] Silvestri LJ, Hurst RE, Simpson L, Settine JM. Analysis of sulfate in complex carbohydrates. Anal Biochem 1982;123:303–9. https://doi.org/10.1016/0003-2697(82)90450-X.

[19] Sun M-L, Zhao F, Shi M, Zhang X-Y, Zhou B-C, Zhang X-Y, et al. Characterization and biotechnological potential analysis of a new exopolysaccharide from the Arctic marine bacterium *Polaribacter* sp. SM1127. Sci Rep 2015;5:18435. https://doi.org/10.1038/srep18435.

[20] Kumar AS, Mody K, Jha B. Bacterial exopolysaccharides – a perception. J Basic Microbiol 2007;47:103–17. https://doi.org/10.1002/jobm.200610203.

[21] Kanmani P, Satish kumar R, Yuvaraj N, Paari KA, Pattukumar V, Arul V. Production and purification of a novel exopolysaccharide from lactic acid bacterium *Streptococcus phocae* PI80 and its functional characteristics activity *in vitro*. Bioresour Technol 2011;102:4827–33. https://doi.org/10.1016/j.biortech.2010.12.118.

[22] Liu J, Luo J, Ye H, Sun Y, Lu Z, Zeng X. Production, characterization and antioxidant activities in vitro of exopolysaccharides from endophytic bacterium *Paenibacillus polymyxa* EJS-3. Carbohydr Polym 2009;78:275–81. https://doi.org/10.1016/j.carbpol.2009.03.046.

[23] Liang Y, Feng Z, Yesuf J, Blackburn JW. Optimization of growth medium and enzyme assay conditions for crude cellulases produced by a novel thermophilic and cellulolytic bacterium, *Anoxybacillus* sp. 527. Appl Biochem Biotechnol 2010;160: 1841–52. https://doi.org/10.1007/s12010-009-8677-x.

[24] Adesulu-Dahunsi AT, Sanni AI, Jeyaram K, Ojediran JO, Ogunsakin AO, Banwo K. Extracellular polysaccharide from *Weissella confusa* OF126: production, optimization, and characterization. Int J Biol Macromol 2018;111:514–25. https://doi.org/10.1016/j.ijbiomac.2018.01.060.

[25] Adesulu-Dahunsi AT, Jeyaram K, Sanni AI, Banwo K. Production of exopolysaccharide by strains of Lactobacillus plantarum YO175 and OF101 isolated from traditional fermented cereal beverage. PeerJ 2018;6:e5326. https://doi.org/10.7717/peerj.5326.

[26] Ismail B, Nampoothiri KM. Production, purification and structural characterization of an exopolysaccharide produced by a probiotic *Lactobacillus plantarum* MTCC 9510. Arch Microbiol 2010;192:1049–57. https://doi.org/10.1007/s00203-010-0636-y.

[27] Lin Y, Liu J, Hu Y, Song X, Zhao Y. An antioxidant exopolysaccharide devoid of pro-oxidant activity produced by the soil bacterium *Bordetella* sp. B4. Bioresour Technol 2012;124:245–51. https://doi.org/10.1016/j.biortech.2012.05.145.

[28] Degeest B, De Vuyst L. Indication that the nitrogen source influences both amount and size of exopolysaccharides produced by *Streptococcus thermophilus* LY03 and modelling of the bacterial growth and exopolysaccharide production in a complex medium. Appl Environ Microbiol 1999;65:2863–70. https://doi.org/10.1128/AEM.65.7.2863-2870.1999.

[29] Mao X-B, Eksriwong T, Chauvatcharin S, Zhong J-J. Optimization of carbon source and carbon/nitrogen ratio for cordycepin production by submerged cultivation of medicinal mushroom *Cordyceps militaris*. Process Biochem 2005;40:1667–72. https://doi.org/10.1016/j.procbio.2004.06.046.

[30] Tang YJ, Sapra R, Joyner D, Hazen TC, Myers S, Reichmuth D, et al. Analysis of metabolic pathways and fluxes in a newly discovered thermophilic and ethanol-tolerant *Geobacillus* strain. Biotechnol Bioeng 2008;102:1377–86. https://doi.org/10.1002/bit.22181.

[31] Xiao Z, Wang X, Huang Y, Huo F, Zhu X, Xi L, et al. Thermophilic fermentation of acetoin and 2,3-butanediol by a novel *Geobacillus* strain. Biotechnol Biofuels 2012; 5(88). https://doi.org/10.1186/1754-6834-5-88.

[32] Smerilli M, Neureiter M, Wurz S, Haas C, Frühauf S, Fuchs W. Direct fermentation of potato starch and potato residues to lactic acid by *Geobacillus stearothermophilus* under non-sterile conditions. J Chem Technol Biotechnol 2015;90:648–57. https://doi.org/10.1002/jctb.4627.

[33] Bibra M, Kunreddy RV, Sani KR. Thermostable xylanase production by *Geobacillus* sp. Strain DUSELR13, and its application in ethanol production with lignocellulosic biomass. Microorganisms 2018:6. https://doi.org/10.3390/microorganisms6030093.

[34] Manca MC, Lama L, Improta R, Esposito E, Gambacorta A, Nicolaus B. Chemical composition of two exopolysaccharides from *Bacillus thermoantarcticus*. Appl Environ Microbiol 1996;62:3265.

[35] Nicolaus B, Panico A, Manca MC, Lama L, Gambacorta A, Maugeri T, et al. A thermophilic *Bacillus* isolated from an Eolian shallow hydrothermal vent able to produce exopolysaccharides. Syst Appl Microbiol 2000;23:426–32. https://doi.org/10.1016/S0723-2020(00)80074-0.

[36] Jain RM, Mody K, Mishra A, Jha B. Isolation and structural characterization of biosurfactant produced by an alkaliphilic bacterium *Cronobacter sakazakii* isolated from oil contaminated wastewater. Carbohydr Polym 2012;87:2320–6. https://doi.org/10.1016/j.carbpol.2011.10.065.

[37] Gómez-Ordóñez E, Rupérez P. FTIR-ATR spectroscopy as a tool for polysaccharide identification in edible brown and red seaweeds. Food Hydrocoll 2011;25: 1514–20. https://doi.org/10.1016/j.foodhyd.2011.02.009.

[38] Radchenkova N, Boyadzhieva I, Atanasova N, Poli A, Finore I, Di Donato P, et al. Extracellular polymer substance synthesized by a halophilic bacterium *Chromohalobacter canadensis* 28. Appl Microbiol Biotechnol 2018;102:4937–49. https://doi.org/10.1007/s00253-018-8901-0.

[39] Zhao S, Cao F, Zhang H, Zhang L, Zhang F, Liang X. Structural characterization and biosorption of exopolysaccharides from *Anoxybacillus* sp. R4-33 isolated from radioactive radon hot spring. Appl Biochem Biotechnol 2014;172:2732–46. https://doi.org/10.1007/s12010-013-0680-6.

[40] Chen Y, Mao W, Tao H, Zhu W, Qi X, Chen Y, et al. Structural characterization and antioxidant properties of an exopolysaccharide produced by the mangrove endophytic fungus *Aspergillus* sp. Y16. Bioresour Technol 2011;102:8179–84. https://doi.org/10.1016/j.biortech.2011.06.048.

[41] Boulet JC, Williams P, Doco T. A Fourier transform infrared spectroscopy study of wine polysaccharides. Carbohydr Polym 2007;69:79–85. https://doi.org/10.1016/j.carbpol.2006.09.003.

[42] Badireddy AR, Chellam S, Gassman PL, Engelhard MH, Lea AS, Rosso KM. Role of extracellular polymeric substances in bioflocculation of activated sludge microorganisms under glucose-controlled conditions. Water Res 2010;44:4505–16. https://doi.org/10.1016/j.watres.2010.06.024.

[43] Cambi A, Netea MG, Mora-Montes HM, Gow NAR, Hato SV, Lowman DW, et al. Dendritic cell interaction with *Candida albicans* critically depends on N-linked mannan. J Biol Chem 2008;283:20590–9. https://doi.org/10.1074/jbc.M709334200.

[44] Jayamanohar J, Devi PB, Kavitake D, Rajendran S, Priyadarisini VB, Shetty PH. Characterization of α-D-glucan produced by a probiont *Enterococcus hirae* KX577639 from feces of south Indian Irula tribals. Int J Biol Macromol 2018;118: 1667–75. https://doi.org/10.1016/j.ijbiomac.2018.07.015.

[45] Lundborg M, Widmalm G. Structural analysis of glycans by NMR chemical shift prediction. Anal Chem 2011;83:1514–7. https://doi.org/10.1021/ac1032534.

[46] Mandal SK, Singh RP, Patel V. Isolation and characterization of exopolysaccharide secreted by a toxic dinoflagellate, Amphidinium carterae hulburt 1957 and its probable role in harmful algal blooms (HABs). Microb Ecol 2011;(62):518–27. https://doi.org/10.1007/s00248-011-9852-5.

[47] Zhang A, Deng J, Yu S, Zhang F, Linhardt RJ, Sun P. Purification and structural elucidation of a water-soluble polysaccharide from the fruiting bodies of the *Grifola frondosa*. Int J Biol Macromol 2018;115:221–6. https://doi.org/10.1016/j.ijbiomac.2018.04.061.

[48] Chen J, Liu C, Chen Y, Chen Y, Chang PR. Structural characterization and properties of starch/konjac glucomannan blend films. Carbohydr Polym 2008;74: 946–52. https://doi.org/10.1016/j.carbpol.2008.05.021.

[49] Das D, Baruah R, Goyal A. A food additive with prebiotic properties of an α-d-glucan from *Lactobacillus plantarum* DM5. Int J Biol Macromol 2014;69:20–6. https://doi.org/10.1016/j.ijbiomac.2014.05.029.

[50] Mishra A, Kavita K, Jha B. Characterization of extracellular polymeric substances produced by micro-algae Dunaliella salina. Carbohydr Polym 2011;83:852–7. https://doi.org/10.1016/j.carbpol.2010.08.067.

[51] Singh RP, Shukla MK, Mishra A, Kumari P, Reddy CRK, Jha B. Isolation and characterization of exopolysaccharides from seaweed associated bacteria Bacillus licheniformis. Carbohydr Polym 2011;84:1019–26. https://doi.org/10.1016/j.carbpol.2010.12.061.

[52] Bhat B, Bajaj BK. Hypocholesterolemic and bioactive potential of exopolysaccharide from a probiotic Enterococcus faecium K1 isolated from kalarei. Bioresour Technol 2018;254:264–7. https://doi.org/10.1016/j.biortech.2018.01.078.

[53] Guo W, Duan J, Geng W, Feng J, Wang S, Song C. Comparison of medium-chain-length polyhydroxyalkanoates synthases from Pseudomonas mendocina NK-01 with the same substrate specificity. Microbiol Res (Pavia) 2013;168:231–7. https://doi.org/10.1016/j.micres.2012.11.003.

[54] Küçükaşik F, Kazak H, Güney D, Finore I, Poli A, Yenigün O, et al. Molasses as fermentation substrate for levan production by *Halomonas* sp. Appl Microbiol Biotechnol 2011;89:1729–40. https://doi.org/10.1007/s00253-010-3055-8.

[55] Arena A, Maugeri TL, Pavone B, Iannello D, Gugliandolo C, Bisignano G. Antiviral and immunoregulatory effect of a novel exopolysaccharide from a marine thermotolerant *Bacillus licheniformis*. Int Immunopharmacol 2006;6:8–13. https://doi.org/10.1016/j.intimp.2005.07.004.

[56] Gugliandolo C, Spanò A, Lentini V, Arena A, Maugeri TL. Antiviral and immunomodulatory effects of a novel bacterial exopolysaccharide of shallow marine vent origin. J Appl Microbiol 2013;116:1028–34. https://doi.org/10.1111/jam.12422.

[57] Bai Y, Zhang P, Chen G, Cao J, Huang T, Chen K. Macrophage immunomodulatory activity of extracellular polysaccharide (PEP) of Antarctic bacterium *Pseudoaltermonas* sp.S-5. Int Immunopharmacol 2012;12:611–7. https://doi.org/10.1016/j.intimp.2012.02.009.

[58] Kothari D, Tingirikari JMR, Goyal A. *In vitro* analysis of dextran from *Leuconostoc mesenteroides* NRRL B-1426 for functional food application. Bioact. Carbohydr Diet Fibre 2015;6:55–61. https://doi.org/10.1016/j.bcdf.2015.08.001.

[59] Das D, Goyal A. Characterization and biocompatibility of glucan: a safe food additive from probiotic *Lactobacillus plantarum* DM5. J Sci Food Agric 2014;94:683–90. https://doi.org/10.1002/jsfa.6305.

[60] You L, Gao Q, Feng M, Yang B, Ren J, Gu L, et al. Structural characterisation of polysaccharides from *Tricholoma matsutake* and their antioxidant and antitumour activities. Food Chem 2013;138:2242–9. https://doi.org/10.1016/j.foodchem.2012.11.140.

[61] Xiao D, Yu S, Xiao J. Antioxidant activities of alkali-soluble polysaccharides from medicinal mushroom *Cordyceps taii* and its chemical characteristics. Biomed Res 2016;27:199–206.

[62] Asker M, Mahmoud MG, Ibrahim AY, Mohamed SS. Inhibitory effect of exopolysaccharide from *Achromobacter piechaudii* NRC2 against cyclooxygenases and acetylcholinesterase with evaluation of its antioxidant properties and structure elucidation. Der Pharm Lett 2015;7:129–41.